A transit-amplifying population underpins the efficient regenerative capacity of the testis

Claudia Carrieri,[1,2] Stefano Comazzetto,[2] Amit Grover,[3] Marcos Morgan,[1,2] Andreas Buness,[2] Claus Nerlov,[3] and Dónal O'Carroll[1,2]

[1]MRC Centre for Regenerative Medicine, Institute for Stem Cell Research, School of Biological Sciences, University of Edinburgh, Edinburgh EH16 4UU, Scotland, UK
[2]European Molecular Biology Laboratory, Mouse Biology Unit, Monterotondo Scalo 00015, Italy
[3]Weatherall Institute of Molecular Medicine, University of Oxford, John Radcliffe Hospital, Headington, Oxford OX3 9DS, England, UK

The spermatogonial stem cell (SSC) that supports spermatogenesis throughout adult life resides within the GFRα1-expressing A type undifferentiated spermatogonia. The decision to commit to spermatogenic differentiation coincides with the loss of GFRα1 and reciprocal gain of Ngn3 (Neurog3) expression. Through the analysis of the piRNA factor *Miwi2* (*Piwil4*), we identify a novel population of Ngn3-expressing spermatogonia that are essential for efficient testicular regeneration after injury. Depletion of *Miwi2*-expressing cells results in a transient impact on testicular homeostasis, with this population behaving strictly as transit amplifying cells under homeostatic conditions. However, upon injury, *Miwi2*-expressing cells are essential for the efficient regenerative capacity of the testis, and also display facultative stem activity in transplantation assays. In summary, the mouse testis has adopted a regenerative strategy to expand stem cell activity by incorporating a transit-amplifying population to the effective stem cell pool, thus ensuring rapid and efficient tissue repair.

INTRODUCTION

The murine spermatogonial stem cell (SSC) resides within the undifferentiated A-type spermatogonia that are defined by A_{single} (A_s, isolated cells), A_{paired} (A_{pr}, chain of two connected cells), and $A_{aligned}$ (A_{al}, chains of 4, 8, or 16 cells) cells. These chains arise because, upon division, spermatogonia often fail to complete cytokinesis and remain connected by intercellular bridges. The A_s stem cell model posits that A_s represented the SSC, given that they reside at the apex of type A undifferentiated spermatogonia (Huckins, 1971; Oakberg, 1971). However, recent data have led to an expanded A_s model wherein the cell surface receptor GFRα1 identifies a subpopulation of A_s, A_{pr}, and A_{al4} (chain of four cells) cells that support long-term spermatogenic homeostasis in mice (Nakagawa et al., 2010; Hara et al., 2014). The GFRα1-positive cells are not an homogeneous population, as *Id4* and *Pax7* marks subsets of A_s, and these populations are endowed with SSC activity (Aloisio et al., 2014; Chan et al., 2014; Sun et al., 2015; Helsel et al., 2017). The relationship between the respective populations remains to be determined, but GFRα1-expression encompasses murine SSCs. Thereafter, SSCs down-regulate GFRα1 and express the transcription factor Ngn3 (Neurog3), which signifies the entry into an intermediate population of primitive spermatogonia that are competent to respond to retinoic acid and differentiate (Nakagawa et al., 2010; Ikami et al., 2015). Interestingly, this Ngn3-positive population acts as a transit-amplifying population under homeostatic conditions (Nakagawa et al., 2007). These Ngn3 potential SSCs can contribute to the pool of GFRα1-positive cells during regeneration (Nakagawa et al., 2010); however, the importance of this phenomenon to the regenerative capacity of the testis remains unknown. After the A_{al8-16} stage, cells up-regulate the surface receptor c-kit to become differentiating spermatogonia that will undergo several further rounds of cell division and are committed to terminal differentiation (Yoshinaga et al., 1991). Here, we sought to identify novel spermatogonial populations and reveal their contribution to testicular physiology.

RESULTS AND DISCUSSION

Miwi2 expression defines a population of adult spermatogonia

Among the loci required for the maintenance of spermatogenesis, the gene encoding the Piwi protein Miwi2 caught our attention due to the slow progressive loss of germ cell phenotype observed in $Miwi2^{-/-}$ mice (Carmell et al., 2007; De Fazio et al., 2011). In addition, Miwi2's reported expression domain is restricted to fetal gonocytes rather than a population of adult spermatogonia (Aravin et al., 2008; Kuramochi-Miyagawa et al., 2008). We therefore reasoned that Miwi2 could also be expressed in a tiny population of adult spermatogonia with SSC activity that has been overlooked by virtue of its rarity. To test this hypothesis, we generated a transcriptional reporter ($Miwi2^{Tom}$) allele whereby the gene encoding the fluorescent tdTomato protein was knocked into the first coding exon of *Miwi2*. tdTomato faithfully recapitu-

Correspondence to Dónal O'Carroll: donal.ocarroll@ed.ac.uk

Abbreviations used: A_{al}, $A_{aligned}$; A_s, A_{single}; A_{pr}, A_{paired}; DTR, diphtheria toxin receptor; DTx, diphtheria toxin; SSC, spermatogonial stem cell.

The Rockefeller University Press $30.00
J. Exp. Med. 2017 Vol. 214 No. 6 1631–1641
https://doi.org/10.1084/jem.20161371

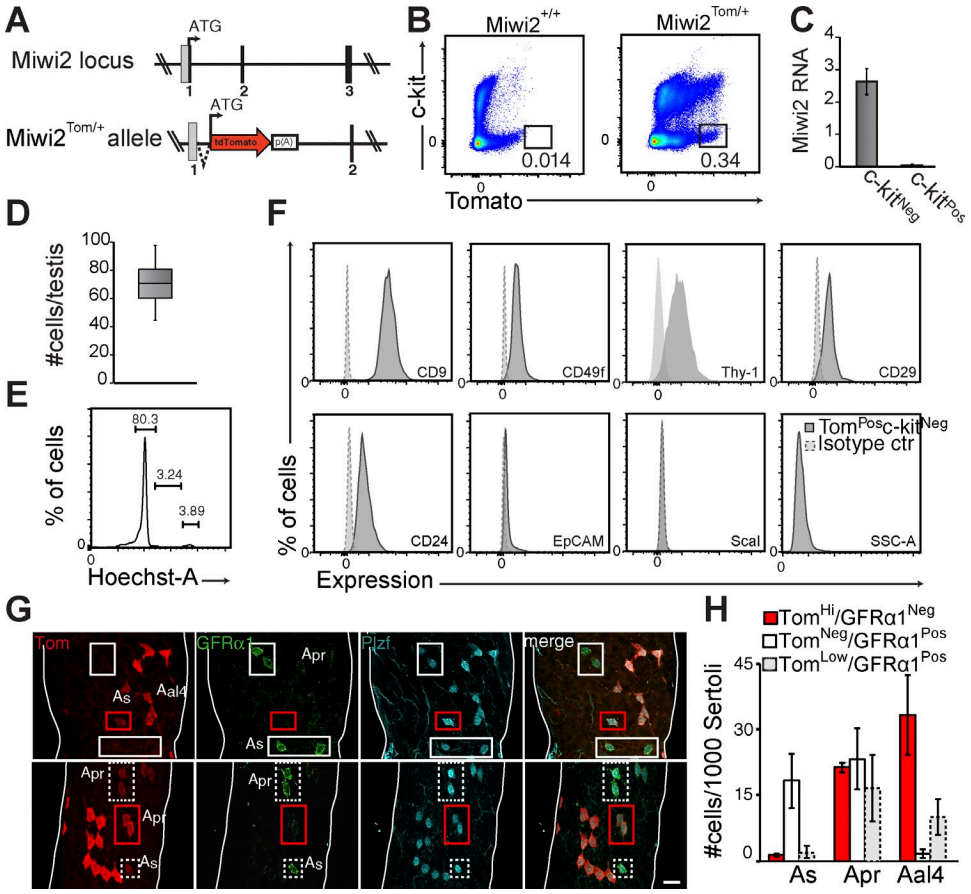

Figure 1. **Miwi2 Tomato expression defines a small population of undifferentiated spermatogonia.** (A) Schematic over of the 5′ region of the Miwi2 locus (top) and the *Miwi2*^{Tom} transcriptional reporter allele (bottom). (B) Representative FACS analysis of live CD45^{Neg} CD51^{Neg} gated cells in testicular populations of wild-type and Miwi2$^{Tom/+}$ mice. Numbers indicate the percentages of cells of the defined subpopulations. (C) qRT-PCR expression analysis of Miwi2 in Miwi2-Tom^{Pos} c-kit^{Neg} and Miwi2-Tom^{Pos} c-kit^{Pos} populations (n = 3). (D) Enumeration of testicular CD45^{Neg} CD51^{Neg} Miwi2-Tom^{Pos} c-kit^{Neg} cells per testis is shown (n = 15). (E) Cell cycle parameters of CD45^{Neg} CD51^{Neg} Miwi2-Tom^{Pos} c-Kit^{Neg} cells as determined by DNA content. (F) Cell surface expression by FACS of the indicated markers in CD45^{Neg} CD51^{Neg} Miwi2-Tom^{Pos} c-Kit^{Neg} are shown, as well as isotype control staining. (G) Representative images of Miwi2$^{Tom/+}$ seminiferous tubules stained with α-GFRα1 (Green), α-tdTomato (Red), and α-Plzf (Blue). Representative examples of Miwi2-Tom^{Hi} GFRα1^{Neg} (red box), Miwi2-Tom^{Neg} GFRα1^{Pos} (green box), and Miwi2-Tom^{Lo} GFRα1^{Pos} (white box) populations are highlighted. Bar, 25 µm. (H) Enumeration of testicular the populations defined in G. Numbers represents total PLZF^{Pos} cells in each category normalized to 1,000 sertoli cells (n = 5). Error bars represent SEM.

lates the expression of Miwi2 in Miwi2$^{+/Tom}$ reprogramming gonocytes (Fig. 1 A and S1 C). Next, we examined by flow cytometry Miwi2-tdTomato (Miwi2-Tom) expression in the testis gating out somatic populations with CD45 and CD51, we observed a tiny tdTomato-positive c-kit–negative (Miwi2-Tom^{Pos} c-kit^{Neg}) population (Fig. 1 B) and a larger c-kit–positive (Miwi2-Tom^{Pos} c-kit^{Pos}) population that constitute proliferating EpCAM-positive differentiating spermatogonia (Fig. S1, E and F). Sorting of these respective populations revealed Miwi2 transcript in the Miwi2-Tom^{Pos} c-kit^{Neg}, but not in the Miwi2-Tom^{Pos} c-kit^{Pos} populations (Fig. 1 C). We therefore concluded that the tdTomato expression in Miwi2-Tom^{Pos} c-kit^{Pos} population reflects the extended life of the tdTomato protein rather than the active expression of the *Miwi2* gene itself. c-kit negativity is a hallmark of SSC populations, we therefore focused our attention on the Miwi2-Tom^{Pos} c-kit^{Neg} population that represents ∼70,000 mostly quiescent or very slowly cycling cells per testis (Fig. 1, D and E). We next sought to define the surface phenotype of Miwi2-Tom^{Pos} c-kit^{Neg} cells, this population uniformly expresses all surface markers (CD9, CD49f, Thy-1, CD29, CD24, and SSC^{lo}) that enrich SSC activity in transplantation assays (Shinohara et al., 1999, 2000; Kubota et al., 2003; Kanatsu-Shinohara et al., 2004; Reding et al., 2010), whereas it is also negative for Sca1 (Fig. 1 F), whose expression has been shown to deplete for SSC potential (Kubota et al., 2003).

We next sought to relate our Miwi2-Tom^{Pos} c-kit^{Neg} population to GFRα1-expressing SSCs, as well as Plzf expression that encompasses a larger population of c-kit negative spermatogonial precursor cells (SPCs; Buaas et al., 2004; Costoya et al., 2004; Hobbs et al., 2010). All Miwi2-Tom^{Pos} c-kit^{Neg} cells were Plzf^{+} (Fig. 1 G). Analysis of GFRα1 and

Tomato expression in A_s, A_{pr}, and A_{al4} revealed three distinct populations of Miwi2-Tomato– and GFRα1-expressing cells, the first group were positive for Miwi2-tdTomato only (Miwi2-Tom^{Hi} GFRα1^{Neg}), the second class was solely GFRα1^{+} (Miwi2-Tom^{Neg} GFRα1^{Pos}), and the third subset expressed low amounts of Miwi2-tdTomato, but were GFRα1^{+} (Miwi2-Tom^{Lo} GFRα1^{Pos}; Fig. 1 G). The majority of A_s were Miwi2-Tom^{Neg} GFRα1^{Pos}, with the other two populations present but contributing minimally (Fig. 1 H). An increased frequency of the Miwi2-Tom^{Hi} GFRα1^{Neg} and Miwi2-Tom^{Lo} GFRα1^{Pos} populations was observed with roughly all three groups contributing equally to A_{pr} spermatogonia (Fig. 1 H). At the A_{al4} stage, the majority of cells had lost GFRα1 expression, and the Miwi2-Tom^{Hi} GFRα1^{Neg} dominated this population (Fig. 1 H). These data suggested that high levels of Miwi2-Tom expression could be used to define a population of GFRα1^{-} spermatogonia. Indeed, FACS analysis of Miwi2-Tom^{Hi} c-kit^{Neg} cells revealed their GFRα1 negativity, with increasing GFRα1 expression in Miwi2-Tom low to dull cells (Fig. S1 G). In summary, Miwi2-Tom^{Hi} c-kit^{Neg} defines a population of GFRα1^{-} undifferentiated spermatogonia that constitute ∼35,000 cells per testis (Fig. S1 H).

Miwi2-expressing cells represent a novel subpopulation of Ngn3^{+} undifferentiated spermatogonia

To further explore the molecular identity of Miwi2-Tom^{Hi} c-kit^{Neg} spermatogonia, we performed gene expression analyses. To this end, we also used the surface expression of CD9 as an additional sorting parameter, as it aids in eliminating contaminating autofluorescent cells from the tiny Miwi2-Tom^{Hi} c-kit^{Neg} population. Comparative gene expression analysis between Miwi2-Tom^{Hi} c-kit^{Neg} population and their Miwi2-Tom^{Hi} c-kit^{Pos} descendants revealed enrichment for many genes that have been associated with SSC/SPC phenotype or function (e.g., Bcl6b, Lin28a, Plzf, Ret, Etv5, and Nanos2) in the Miwi2-Tom^{Hi} c-kit^{Neg} population (Buaas et al., 2004; Costoya et al., 2004; Chen et al., 2005; Naughton et al., 2006; Oatley et al., 2006; Sada et al., 2009; Zheng et al., 2009; Fig. 2, A and B). Interestingly, the Miwi2-Tom^{Hi} c-kit^{Neg} population also expressed Ngn3 that is associated with transit amplification and acquisition of differentiation competence under homeostatic conditions (Nakagawa et al., 2010; Ikami et al., 2015). To further define the Miwi2-Tom^{Hi} c-kit^{Neg} spermatogonial population, we performed single-cell qRT-PCR analysis using a panel of SSC, SPC, and differentiating spermatogonia markers (Fig. 2 C). Analysis of Miwi2-Tom^{Hi} c-kit^{Pos} differentiating spermatogonia validated this approach with cells being negative for GFRα1, Miwi2, Nanos2, and Nanos3 while expressing c-kit mRNA (Fig. 2 C). Miwi2-Tom^{Hi} c-kit^{Neg} cells showed a distinct heterogeneity, with a small population registering positive for c-kit mRNA (Fig. 2 C), we posit that this cellular population is in the process of committing to differentiation and start to express mRNA but is not yet positive for the encoded protein. All Miwi2-Tom^{Hi} c-kit^{Neg} cells express the undifferentiated spermatogonia markers, Plzf, Lin28 and Oct4. Within the Miwi2-Tom^{Hi} c-kit^{Neg} population, a few cells express the GFRα1 mRNA although these cells are negative for expression of the protein. Most importantly all Miwi2-Tom^{Hi} c-kit^{Neg} cells expressed Ngn3 at the single cell level. To understand the overlap between Miwi2-Tom^{Hi} c-kit^{Neg} and Ngn3^{Pos} populations, we generated Miwi2$^{+/TOM}$; Ngn3^{GFP} Tg^{+} mice. Miwi2-Tom^{Hi} c-kit^{Neg} cells constituted a sub-population of Ngn3^{Pos} spermatogonia (Fig. 2, D and E). The fraction of Ngn3^{Pos} (GFRα1^{Neg}) cells that express Miwi2-Tom increases with chain length and by A_{al8} stage all chains are positive for both Miwi2 and Ngn3 (Fig. 2, F and G). In summary, Miwi2 expression identifies a novel subpopulation of Ngn3^{+} undifferentiated spermatogonia.

Miwi2-expressing spermatogonia are transit-amplifying cells under homeostatic conditions

To determine the contribution of this novel Miwi2-Tom^{Hi} c-kit^{Neg} population to steady state or the long-term maintenance of spermatogenesis we opted for a lineage ablation strategy (Saito et al., 2001). To this end, the gene encoding the diphtheria toxin receptor (DTR) was placed into the Miwi2 locus (*Miwi2^{DTR}* allele; Fig. 3 A and S2 A), thus enabling diphtheria toxin (DTx)-mediated lineage ablation experiments. Unfortunately, the DTR antibody did not work for whole mount immunostaining, such that we could not resolve the DTR-expressing cells at the cellular A_s-A_{al} resolution. However, DTR expression was determined by FACS and was restricted to a tiny population of CD45^{Neg} CD51^{Neg} c-kit^{Neg} (Miwi2-DTR^{Pos} c-kit^{Neg}) cells, but not in any c-kit^{Pos} population within Miwi2$^{+/DTR}$ testis (Fig. 3 B, top). Importantly, the overall percentages and numbers of Miwi2-DTR^{Pos} c-kit^{Neg} and Miwi2-Tom^{HI} c-kit^{Neg} were roughly equivalent (Fig. S1 H and S2 C). We administered three DTx doses spaced 2 d apart and analyzed 1 d after the last injection, here the Miwi2-DTR^{Pos} c-kit^{Neg} population was reduced close to background levels (Fig. 3 B, bottom). This acute loss of Miwi2-DTR^{Pos} c-kit^{Neg} population had no impact on GFRα1-expressing SSC populations (Fig. 3 C); however, strikingly, most differentiating spermatogonia (CD45^{Neg} CD51^{Neg} c-kit^{Pos}) were absent (Fig. 3 B, bottom). We interpreted this loss of c-kit^{Pos} cells as the failure to replenish the differentiating spermatogonia population upon their differentiation into meiocytes, and histological analysis supported this (Fig. 3 D). Indeed, a single administration of DTx and analysis 1 d after the injection revealed that the Miwi2-DTR^{Pos} c-kit^{Neg} population was reduced, but without affecting other testicular populations inclusive of the c-kit^{Pos} populations (Fig. S2 D). We next followed the consequence of Miwi2-DTR^{Pos} c-kit^{Neg} depletion on spermatogenesis over time. A single wave of spermatogenesis was lost in the Miwi2$^{DTR/+}$ DTx-treated mice, with testicular weight being reduced by ∼30% 6 wk after injection, but recovering fully by 16 wk (Fig. 3, E and F). Concomitantly, fertility was lost at 6 wk and regained at 12 wk after DTx injection in the Miwi2$^{DTR/+}$ mice (Fig. 3 G). Additionally, the reappearance of

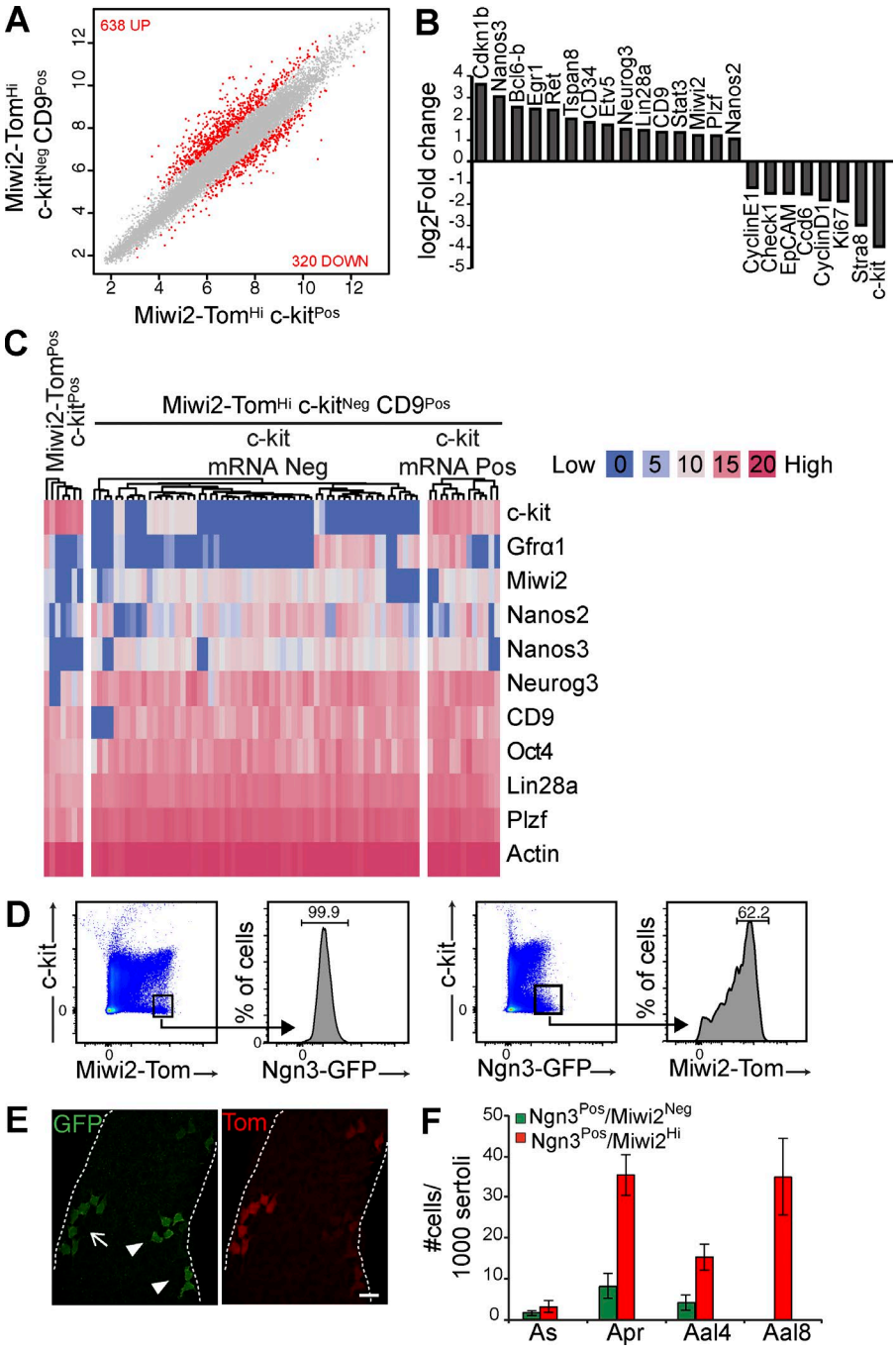

Figure 2. **Miwi2-Tom^{Hi} c-Kit^{Neg} cells are a subpopulation of Ngn3-positive spermatogonia.** (A) Scatter plot of gene expression from biological quadruplicates of CD45^{Neg} CD51^{Neg} Miwi2-Tom^{Pos} c-Kit^{Neg} (n = 4) and CD45^{Neg} CD51^{Neg} Miwi2-Tom^{Pos} c-Kit^{Pos} populations (n = 4). Genes highlighted in red show a fold change ≥2 and a significance of ≤0.05. Number of genes up- and down-regulated in the respective populations are indicated. (B) Enrichment and depletion of select genes in CD45^{Neg} CD51^{Neg} Miwi2-Tom^{Pos} c-Kit^{Neg} population. (C) Fluidigm qRT-PCR of Miwi2-Tom^{Pos} cells as indicated. Each row corresponds to a specific gene; each column corresponds to a single cell; color code of expressions levels indicated in $\log_2$ expression. (D) Representative FACS analysis of testicular cells from Miwi2$^{Tom/+}$; Ngn3$^{GFP/+}$ mice. CD45^{Neg} CD51^{Neg} gated cells are shown. Numbers indicate the percentages of cells of the defined subpopulations. (E) Representative images of Miwi2$^{Tom/+}$; Ngn3$^{GFP/+}$ seminiferous tubules stained with α-GFP (green) and α-tdTomato (red). White arrow indicates Miwi2-Tom and Ngn3-GFP double-positive spermatogonia. Solid white arrow indicates Ngn3-GFP single-positive spermatogonia. (F) Enumeration of Ngn3^{Pos} Miwi2^{Neg} GFRα1^{Neg} and Ngn3^{Pos} Miwi2^{Pos} GFRα1^{Neg} cells expressed as number of cells per 1,000 sertoli cells (n = 4). Error bars represent SEM. Bar, 25 µm.

Miwi2-DTR^{Pos} c-kit^{Neg} was observed in Miwi2$^{+/DTR}$ testis 8 wk after DTx treatment (Fig. S2 E). Thus, the Miwi2-DTR^{Pos} c-kit^{Neg} population behaves as transit amplifying population in this assay and the cells within this population are not broadly required for the long-term homeostasis of the testis.

Miwi2-expressing spermatogonia are essential for the efficient regenerative capacity of the testis

Miwi2 is member of the Piwi subclade of the Argonaute family, in planarians the Piwi proteins Smedwi2 and Smedwi3 are expressed in neoblasts and essential for the remarkable regenerative capacity of this organism (Reddien et al., 2005; Palakodeti et al., 2008). Additionally, whereas Ngn3^{+} cells represent transit-amplifying cells under homeostasis, lineage-tracing studies have shown some ability of this population to contribute to the regeneration upon injury (Nakagawa et al., 2007). We therefore sought to understand if the Miwi2-DTR^{Pos} c-kit^{Neg} Ngn3^{Pos} population not only contributes to regeneration but could also be critical for the regenerative capacity of the testis upon injury. Busulfan is a DNA-alkylating agent

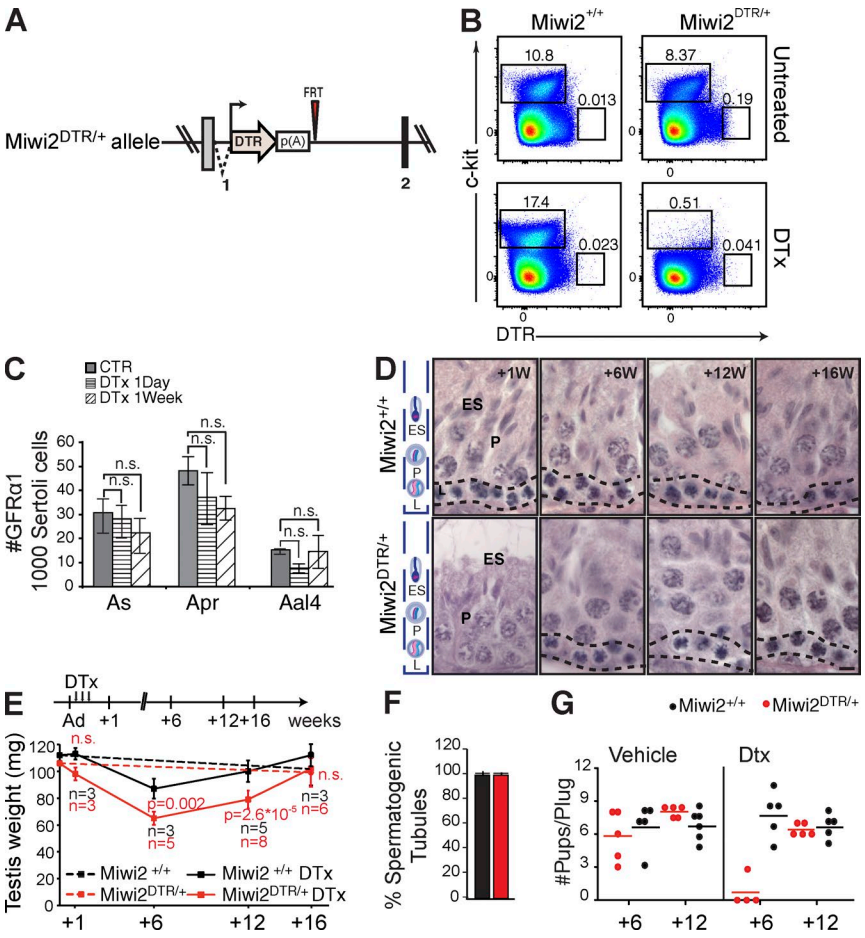

Figure 3. **Miwi2-expressing cells are transit amplifying and do not contribute to the long-term maintenance of spermatogenesis.** (A) Schematic overview of the *Miwi2*^{DTR} allele. (B) Representative FACS analysis of live CD45^{Neg} CD51^{Neg} gated cells is shown of testicular populations of wild-type and Miwi2$^{DTR/+}$ mice stained with c-kit and DTR antibodies (top) and after 3x DTx administrations analyzed 1 d after the last injection (bottom). Numbers indicate the percentages of cells of the defined subpopulations. (C) Enumeration of the GFRα1^{Pos} populations in adult Miwi2$^{DTR/+}$ mice that were untreated (n = 3) or treated with 3x DTx injections and analyzed 1 d (n = 4) or 1 wk (W; n = 4) after the last injection. Numbers represent cells of indicated chain length normalized to 1,000 sertoli cells. (D) Histology of testis; sections stained with H&E at time points indicated (1–16 wk [W]) after DTx administration are shown. Bar, 10 µm. (E) Testicular weight of the indicated cohorts at indicated time points. n, number of mice analyzed per time point. P-values are shown; n.s., no statistical significance. (F) Enumeration of fully spermatogenic tubules in wild-type and Miwi2$^{DTR/+}$ mice at the final 16 wk time point after DTx administration is shown. (G) Fertility as represented by pups per plug of the indicated cohorts at 6 and 12 wk after DTx or vehicle control injection. Black and red represent wild-type and Miwi2$^{DTR/+}$ Dtx-treated mice, respectively. Error bars represent SEM.

that is particularly toxic to spermatogonia, and at intermediate doses this chemical can be used to damage testis and induce regeneration (van Keulen and de Rooij, 1973). We subjected a cohort of Miwi$^{+/+}$ and Miwi$^{+/DTR}$ adult mice to either vehicle control or 3× DTx injections, immediately followed by treatment of the mice with an intermediate dose of busulfan (Fig. 4 A). The regeneration of vehicle control–injected mice was identical between the wild-type and Miwi2$^{+/DTR}$ genotypes (Fig. 4 B). However, within the cohort where DTx was administered, the Miwi2$^{+/DTR}$ mice failed to recover with the same kinetics as control mice. At 12 wk after busulfan injection, the wild-type mice had reached maximal recovery, whereas the Miwi2$^{+/DTR}$ mice showed little or no recovery at this time point (Fig. 4, B–D). Only at 24 wk after injury did the DTx-injected Miwi2$^{+/DTR}$ mice mount a significant, but far from complete, recovery (Fig. 4, B–D).

A theoretical caveat of the aforementioned experiment is that the acute elimination of the Miwi2-DTR^{Pos} c-kit^{Neg} cells may provoke cell cycle entry in the GFRα1^{Pos} population, rendering these cells more sensitive to busulfan treatment. We therefore did the reciprocal experiment; first inducing damage with busulfan, and then treating with DTx. This strategy resulted in a similar outcome with the Miwi2$^{+/DTR}$ mice, but not control, mice showing defective regeneration (Fig. S3). These data suggest that whereas the Miwi2^{Pos} c-kit^{Neg} population is transit amplifying under homeostatic conditions, they could harbor facultative stem cell ability under stress conditions. To directly test this, we used the transplantation assay,

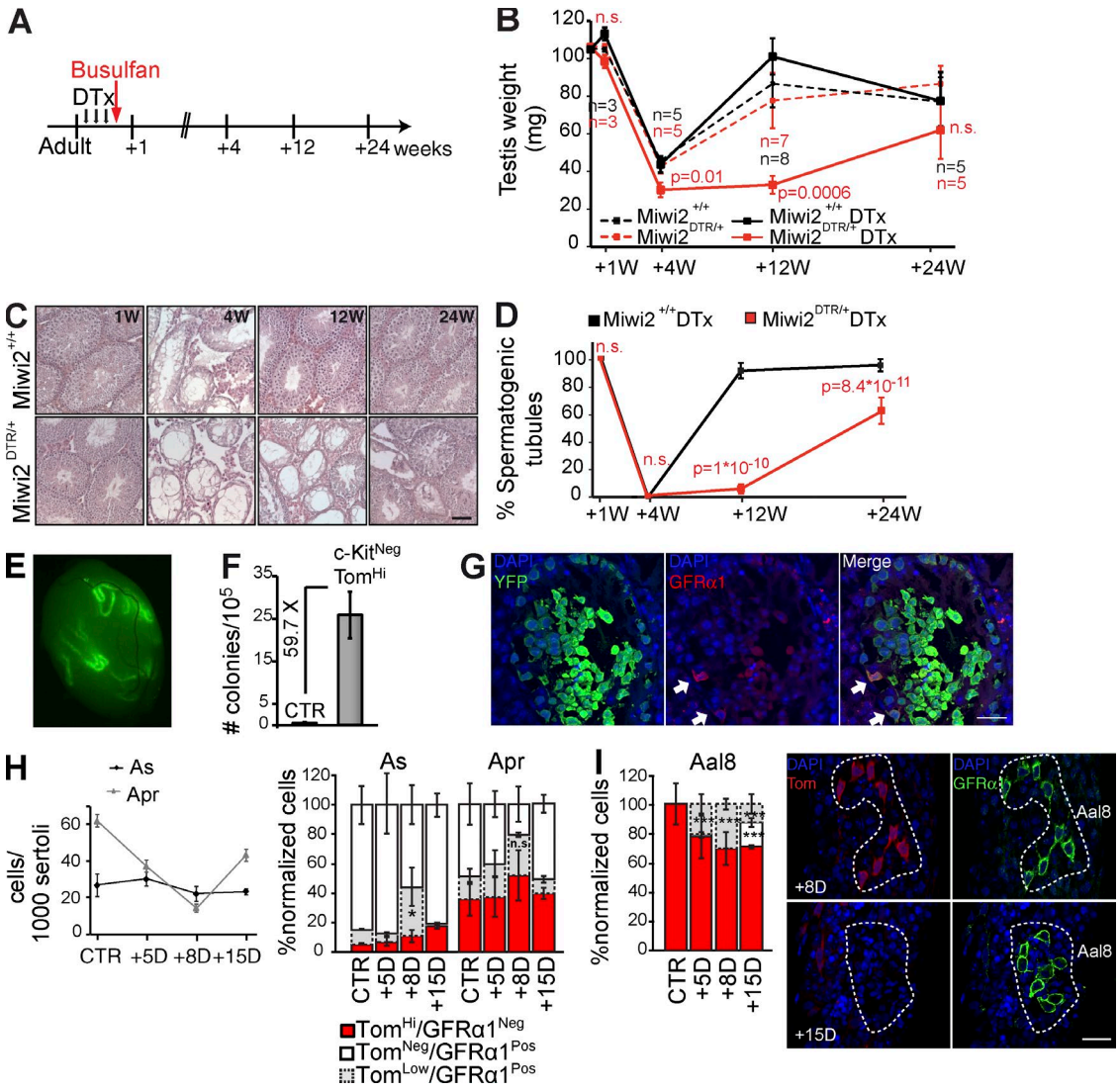

Figure 4. **Miwi2-expressing cells are crucial for the regenerative capacity of the testis after injury.** (A) Experimental overview of DTx and busulfan injections, as well as time points analyzed. (B) Testicular weight of the indicated cohorts overtime is shown. n, number of mice analyzed per time point for the DTx-injected mice. P-values are shown; n.s., no statistical significance. (C) Histology of testis section stained with H&E for the same time points as indicated in A. Bar, 100 µm. (D) Enumeration of fully spermatogenic tubules in DTx-injected wild-type and Miwi$^{DTR/+}$ mice for each stage during the time course (n = 3 for each genotype and time point). P-values are shown; n.s., no statistical significance. (E) Representative image of reconstitution from CD45^{Neg} CD51^{Neg} Miwi2-Tom^{Pos} c-kit^{Neg} transplanted cell isolated from Miwi2$^{Tom/+}$; Rosa26$^{YFP/+}$ mice. Colonies derived from the YFP-positive donor cells are shown. Bar, 1 mm. (F) Quantitation of colony formation for the indicated populations analyzed 3 mo after transplantation. Fold enrichment are calculated as colony forming units normalized per 10^5 cells for the 10^4 sorted CD45^{Neg} CD51^{Neg} Miwi2-Tom^{Pos} c-kit^{Neg} (n = 12) cells and 10^6 testicular control cells transplanted (n = 4). Error bars represent SEM. (G) Immunofluorescence analysis of a transplanted YFP$^+$ colony, spermatogonia that express GFRα1 indicated (white boxes) after reconstitution. Bar, 50 µm (H) Total number of A_s and A_{pr} spermatogonia per 1,000 of sertoli cells before (CTR) and at day 5, 8, and 15 after busulfan treatment (left). Enumeration of Miwi2-Tom^{Hi} GFRα1^{Neg}, Miwi2-Tom^{Neg} GFRα1^{Pos}, and Miwi2-Tom^{Low}GFRα1^{Pos} populations is shown for the same time points (right). Stacked columns represent normalized percentages of the indicated populations per time point. Error bars represent SEM of three (CTR and +15D) and 4 (+5D and +8D) mice analyzed. Significance between CTR and +8D Miwi2-Tom^{Low}GFRα1^{Pos} populations is indicated; *, $P < 0.05$; n.s., $P > 0.05$. (I) Normalized percentages of A_{al8} at indicated time points after busulfan treatment (left) as presented in H. Significance between CTR and the indicated populations is shown; ***, $P < 0.001$. Representative images of Miwi2-Tom^{Low}GFRα1^{Pos} and Miwi2-Tom^{Pos} c-kit^{Neg} A_{al8} are shown for +8D (top) and +15D (bottom), respectively. Bar, 25 µm.

where constitutively YFP-labeled Miwi2-Tom^{Hi} c-kit^{Neg} cells are FACS sorted and transplanted into germ cell–depleted testis. Indeed, the Miwi2-Tom^{Hi} c-kit^{Neg} population contained robust reconstitution activity (Fig. 4, E and F). Collectively, these data demonstrate that the Miwi2-expressing spermatogonial population that normally behaves as transit

amplifying cells has stem cell activity in reconstitution assays and is essential for the efficient regenerative capacity of the testis after injury.

Given that all Miwi2^{Pos} c-kit^{Neg} cells express Ngn3, and Ngn3^{+} spermatogonia have a proven ability to revert to GFRα1-expressing cells (Nakagawa et al., 2010), reversion may represent the mechanism by which Miwi2-expressing spermatogonia contribute to regenerative spermatogenesis. Although we cannot provide the formal proof of lineage tracing to observe the reversion of Miwi2^{Pos} c-kit^{Neg} cells to GFRα1-expressing SSCs, we decided to look for evidence that would support this hypothesis. First, Miwi2^{Pos} c-kit^{Neg} cells can give rise to GFRα1-expressing spermatogonia upon transplantation (Fig. 4 G). Next, we sought to understand whether the behavior of the respective Miwi2 and GFRα1-expressing populations in the early stages of regeneration would be consistent with a reversion mechanism. We examined the acute impact of busulfan on A_s and A_{pr} primitive spermatogonia. Damage to these populations reached a maximum at day 8, with the initiation of recovery observed as early as day 15 after busulfan administration (Fig. 4 H). We then analyzed the fractions of Miwi2-Tom^{Hi} GFRα1^{Neg}, Miwi2-Tom^{Lo} GFRα1^{Pos}, and Miwi2-Tom^{Neg} GFRα1^{Pos} in A_s and A_{pr} populations during this time frame. Strikingly, we saw an increase in the Miwi2-Tom^{Lo} GFRα1^{Pos} A_s population at day 8 that preceded the qualitative recovery in the Miwi2-Tom^{Neg} GFRα1^{Pos} cells at day 15 after damage induction (Fig. 4 H). We also saw the emergence of Miwi2-Tom^{Lo} GFRα1^{Pos} A_{al8} chains at day 5, with the presence of Miwi2-Tom^{Neg} GFRα1^{Pos} observed at day 15 after damage induction; importantly, neither of these A_{al8} populations are observed in homeostatic testis (Fig. 4 I). GFRα1^{Pos} A_{al8} have been observed in regenerating testis (Nakagawa et al., 2010) and could, in theory, also contribute to the quantitative recovery of the A_s GFRα1^{Pos} population through fragmentation of the spermatogonial chains. Given that Miwi2^{Pos} c-kit^{Neg} cells express Ngn3 and can give rise to GFRα1^{Pos} cells in transplantation assays, and the observed expansion of Miwi2-Tom^{Lo} GFRα1^{Pos} cells before the onset of GFRα1^{Pos} cell recovery, it is reasonable to speculate that reversion could be the mechanism by which Miwi2-expressing spermatogonia underpin regenerative spermatogenesis. Interestingly, in the *Drosophila* germline, transit amplifying spermatogonial cells can revert to stem cell identity upon the ablation of germline stem cells (Brawley and Matunis, 2004).

Here, we show that Miwi2-expressing undifferentiated spermatogonia that normally behave as transit-amplifying cells constitute a cellular population that is essential for the efficient regenerative capacity of the testis. These Miwi2-expressing cells constitute a novel subpopulation of Ngn3^{+} spermatogonia. Although Ngn3^{+} spermatogonia are transit amplifying during homeostasis, they have been shown to retain stem cell potential and can contribute to regeneration by transplantation and lineage tracing, respectively (Nakagawa et al., 2007, 2010); however, their relative importance to the regenerative process is not defined. Here, we show by cell ablation that the Miwi2-expressing subpopulation of Ngn3^{+} spermatogonia is crucial for efficient regenerative spermatogenesis. Our data demonstrate that mouse spermatogenesis has adopted a strategy to expand the pool of spermatogonial cells with stem cell activity under regenerative conditions. The intestinal and airway epithelium upon injury adopt a similar strategy, where progenitor cells can dedifferentiate in vivo into stem cells and contribute to repair (van Es et al., 2012; Tata et al., 2013; Metcalfe et al., 2014; Zheng et al., 2014). This regenerative strategy is distinct from hematopoiesis, where repair is mediated by hematopoietic stem cells (Wilson et al., 2008; Buza-Vidas et al., 2009; Busch et al., 2015). The expansion of the effective SSC compartment to incorporate an undifferentiated transit amplifying spermatogonial population affords a protective mechanism ensuring efficient repair. It likely limits the amount of potentially damaging replication cycles that the homeostatic stem cells would be required to undergo to mediate repair, thus also protecting the genomic integrity of the germ line. The sensitivity of SSCs to the chemotherapeutic agents renders male cancer patients sterile; this is particularly acute for prepubescent patients where sperm cannot be frozen for future parenthood needs. Thus, our findings not only identify SSCs but also potentially spermatogonial transit amplifying cells as key target populations for cryopreservation and the basis of an autologous transplantation strategy for the restoration of fertility in cancer survivors.

MATERIALS AND METHODS

Mouse strains

For the Miwi2^{Tom} allele, a targeting construct was generated by recombineering, containing two homology arms to the Miwi2 locus. Within this vector, a synthetic intron and the coding sequence of tdTomato fluorescent protein, followed by bovine growth hormone polyA signal, as well as a *frt*-flanked neomycin (*neo*) cassette for ES-cell screening, was inserted into the starting codon of Miwi2. Southern blotting of the individual ES-cell–derived clones with a Miwi2 exon 3 external probe was used to identify homologous recombinants. Digestion of wild-type genomic DNA from tail biopsies with AseI generates a 9.7-kb DNA fragment; integration of the *neo^{r}-frt* flanked cassette introduces an additional AseI site, thus decreasing the size of the AseI DNA fragment recognized to 4.4-kb in the targeted allele. Flp-mediated recombination and excision of the *neo^{r}-frt* flanked cassette results in a 11.7-kb AseI DNA fragment recognized by the external exon 3 probe, which is diagnostic of the Miwi2^{Tom} allele.

For the Miwi2^{DTR} allele, within recombineered Miwi2 vector that contained the homology arms, a synthetic intron and the membrane-anchored form of human heparin-binding epidermal growth factor-like growth factor (HB-EGF), otherwise termed diphtheria toxin receptor (DTR), followed by BGH polyA signal, a *frt* flanked neomycin (*neo*) cassette was inserted into the starting codon of Miwi2. Southern blotting of the wild-type *Miwi2* locus digested with *AseI* gives

a 9.7-Kb band; Flp-mediated recombination and excision of the *neo*^{r}*-frt* flanked cassette results in an 11-kb AseI DNA fragment recognized by the external exon 3′ probe, which is diagnostic of the *Miwi2*^{DTR} allele. The Miwi2-targeting constructs were electroporated into A9 ES cell (De Fazio et al., 2011). Southern blotting as described for the individual ES-cell–derived clones was used to identify homologous recombinants. A9-targeted ES cells were injected into C57BL/6 8-cell-stage embryos for the generation of fully ES-cell–derived mice (De Fazio et al., 2011). The *Miwi2*$^{tdTomato\text{-}Neo/+}$ and *Miwi2*$^{DTR\text{-}Neo/+}$-targeted mice were then crossed to the FLP-expressing transgenic mice (FLPeR; Farley et al., 2000) to remove the *frt* flanked *neo*^{r} cassette, resulting in the generation of *Miwi2*$^{tdTomato/+}$ and *Miwi2*$^{DTR/+}$ alleles, respectively. The mice analyzed in this study were on a mixed C57BL/6 and 129 genetic background. Primers used for the amplification of the exon 3 probe were Miwi2_Ex3_probe_F 5′-AAGGAAGGATAGTCGCGTGTT-3′ and Miwi2_Ex3_probe_R 5′-ACACCCAACTCTTCGAAGTCC-3′. Common primers used for screening Miwi2^{+}, Miwi2^{Tom}, and Miwi2^{DTR} alleles were Miwi2-Tom_GenoF1 5′-TACTCCCAAACTCCGAGTCAC-3′, Miwi2-Tom_GenoR1 5′-GTGCCTATCAGAAACGCAAGA-3′, and Miwi2-Tom_GenoR2 5′-CTCCTAGCCAGAGTGCCTTTT-3′. All mice were bred and maintained in EMBL Mouse Biology Unit, Monterotondo in accordance with current Italian legislation (Art. 9, 27 January 1992, number 116) under license from the Italian health ministry.

Cell preparation and FACS staining

After the removal of the tunica albuginea, the isolated testes were rinsed twice in DMEM enriched with 1 mM of sodium pyruvate and 1.5 mM of sodium lactate before enzymatic digestion. To achieve the complete single-cell suspension, the tubules were digested first with 0.5 mg/ml of type XI collagenase (c7657; Sigma-Aldrich) at 32°C for 7 min at 700 rpm shaking, followed by 0.05% Trypsin digestion (Gibco) in the presence of 0.05 mg/ml of DNase I (DN-25; Sigma-Aldrich). After digestion, cells are filtered through a 70-µm cell strainer (14–959-49A; Falcon) and subsequently pelleted by centrifugation at 1,000 rpm for 5 min. 5–7 million cells per sample were stained with the fluorophore-conjugated antibodies in PBS 3%/FBS/0.01% sodium azide in ice. For the DTR and GFRα1 FACS staining, cells were incubated with anti-HB EGF (DTR) biotinylated antibody (clone 4G10; R&D System) or α-GFRα1 antibody (Goat-IgG; Neuronics) diluted 1:50 in PBS, 3% FBS, and 0.01% sodium azide and incubated on ice with periodic mixing of the sample every 5 min. After washing in PBS-FBS, cells were then incubated on ice for 30 min with either streptavidin pe-Cy7A (eBioscience 25–0441-82) or 647Alexafuor donkey anti–goat antibody for DTR and GFRα1 staining, respectively. FACS antibodies used in this study were as follows: CD45 (eBioscience; clone A20), CD51 (BioLegend; clone RMV-7); CD90.2 (BioLegend; 30-H12); CD29 (BioLegend; clone hmbeta1-1); CD9 (eBioscience; clone KMC8); CD24 (BioLegend; clone M1/69); CD34 (clone RAM34); CD117 (eBioscience; clone 2B8); Sca-1 (BioLegend; D7); CD49f (eBioscience; clone GoH3); and EpCAM (eBioscience; G8.8), plus isotype controls rat IgG2a, k PE-Cy7 (eBioscience 25–4321-81), rat IgG2a, k, FITC (eBioscience), Rat IgG2a, k, biotinylated (eBioscience), rat IgG2b, k, APC (BD), rat IgG2b, k, and Pacific Blue (BioLegend).

Reverse transcription and quantitative PCR

50 ng of total RNA from FACS-sorted cell populations were reverse transcribed with random hexamer primers using Superscript II Reverse transcription (Invitrogen,18064-022) following manufacturer instructions. A quantitative real-time reaction was performed on a LightCycler 480 PCR instrument (Roche) using 2× SYBR green I master (Roche). All the expression data were normalized to the expression levels of β actin reference gene using the 2-ΔΔCt method (Livak and Schmittgen, 2001). The primers used for qRT PCRn were as follows: Miwi2_FW 5′-CGACCCCGATGTTCAGTT-3′, Miwi2_RV 5′-ATCAATACCCACGACCATCA-3′, β-actin F 5′-CACACCCGCCACCAGTTC-3′, and β-actin R 5′-CCCATTCCCACCATCACACC-3′.

Whole mount immunofluorescence

Tubules were dealbugined with 0.5 mg/ml collagenase in PBS as for FACS preparation and subsequently fixed in 4% paraformaldehyde for 8–12 h at 4°C. After fixation, tubules were quenched in 1 M Glycine for 30 min at room temperature, and then blocked/permeabilized in PBS/0.5% Triton X-100/5% donkey serum/0.5% BSA. Primary antibodies are incubated in PBS/0.5% BSA overnight at room temperature. After washes in PBS, the tubules were incubated with Alexa Fluor 488–, 647–, or 546–conjugated secondary antibodies in PBS/0.5% BSA, 0.1% Triton X-100. The tubules were then counterstained with DAPI (5 µg/ml) and mounted in prolong gold on glass slides. Antibodies used were α-RFP (Rockland), α-GFP (Aves), α-GFRα1 (Neuromics Goat-IgG), α-Plzf (EMD Millipore; mouse monoclonal), and c-kit (R&D Systems; goat polyclonal).

Immunofluorescence staining on tissue sections

Immunofluorescence double staining was performed on fetal testicular tissue samples. Fetal testes were dissected from E12.5 Embryos, fixed in 4% paraformaldehyde for 2 h, and then quickly PBS washed and immersed in cryoprotecting solution PBS/10% sucrose solution for 2 h at 4°C and in following PBS/20% sucrose from 2 h to overnight (until the tissue sinks at the bottom of the −12/tube) at 4°C. Tissues were OCT-embedded and cryosectioned in 7-µm-thick slides. Slides were washed in PBS, permeabilized in PBS/0.1% Triton X-100 for 30 min, blocked with PBS/0.1% Triton X-100/5% donkey serum/0.5% BSA, and incubated o.n. at room temperature with primary antibody in blocking solution without Triton X-100. After washes, Alexa Fluor 488–,

647–, or 546–conjugated secondary antibodies were applied. Nuclei were finally counterstained with DAPI (5 µg/ml) and slides mounted in ProLong Gold antifade reagent (Thermo Fisher Scientific). Antibodies used were as follows: α-RFP (Rockland) and α-GFRα1 (R&D Systems).

Lineage ablation

DTx (Sigma-Aldrich) was dissolved in water to make high-concentration aliquots (1 mg/ml) that were kept as stocks at −80°C. For injections, the concentrated DTx stock was diluted in PBS for the working concentration (5 µg/ml). Miwi2$^{DTR/+}$ mice were injected intraperitoneally three times, every 2 d (unless specified otherwise), with DTx at a concentration of 25 ng/gram of mouse body weight.

Testicular damage and regeneration experiments

Busulfan powder was dissolved in dimethyl sulfoxide (DMSO) prewarmed to 41–43°C. After the busulfan was dissolved, an equal volume of distilled water (41–43°C) was added to make the working solution. Miwi2$^{+/+}$ or Miwi2$^{DTR/+}$ mice were injected once with busulfan at a concentration of 20 mg/kg of mouse body weight as specified in the text. Analysis of regeneration was performed at the time points described in the text and figure legends.

Histology

Testes dissected from Miwi2$^{DTR/+}$ mice were fixed in Bouin's solution (Sigma-Aldrich), embedded in paraffin, and sectioned as follows: approximately six consecutive 7-µm-thick slices were cut and deposited on a glass slide, and then the specimen was trimmed for a total 500 length, this process was repeated twice to get three slides per animal at roughly the beginning, at 1/4, and at 1/2 of the whole testis longitudinal length. Slides were H&E stained and the best section was chosen for 2D image reconstruction using the mosaic function of the Microdissector 7000 microscope (Leica). Tubules from the sections of the testis were classified as normal or aspermatogenic.

Gene expression profiling

Gene expression analysis was performed using the Affymetrix Mouse Gene 2.0 ST Array from total RNA of FACS-sorted CD45^{Neg} CD51^{Neg} Miwi2-Tom^{Pos} c-Kit^{Neg} and CD45^{Neg} CD51^{Neg} Miwi2-Tom^{Pos} c-Kit^{Pos} populations. Biological quadruplicates were processed for each population. Gene expression data are deposited in ArrayExpress (E-MTAB-4828).

Fluidigm qPCR

Fluidigm q-PCR on single-cell–sorted Miwi2-Tom^{Pos} c-kit^{Neg} was performed as previously described in (Grover et al., 2016). TaqMan probes used for this assay were as follows: c-Kit Mm00445212_m1; GFRa1 Mm00439086_m1; Miwi2 Mm01144775_m1; Nanos2 Mm04212806_s1; Nanos3 Mm00808138_m1; Neurog3 Mm00437606_s1; CD9 Mm00514275_g1; OCT-4 Mm03053917_g1; Lin28 Mm00524077_m1; Plzf Mm01176868_m1; and b-actin Mm00607939_s1.

Fluidigm qPCR analysis

The Fluidigm single-cell qPCR gene expression analysis platform was used to quantify transcript levels. Ct values were converted to logarithmic expression levels by the Fluidigm software (SINGuLAR Analysis Toolset 3.0). The limit of detection was set to a Ct value of 28. The software assigns zero expression to Ct values below the detection limit and to failed measurements. Only cells were selected for which the FACS measurement of CD9 exceeds 3000 F.U. and for which the sum of all expression levels exceeds 200. The results for the 11 genes shown in the heat map are based on 22 out of the 26 probes for these genes. Only the best matching probes were used to calculate mean gene expression levels in most cases. Cells are grouped by their c-kit status as measured in the FACS, and then further split into subgroups depending on their c-kit gene expression level while using a threshold of 10. Bioconductor packages and the R software was used for the visualization and clustering based on the similarity of the expression profiles.

Preparation of germ cell–depleted mice as recipients for transplantation

For the elimination of spermatogenesis to generate recipient mice for the transplantation assays, a single 40 mg/kg injection of busulfan was given to 4–5-wk-old C57BL6n male mice. Busulfan powder was prepared as described in Testicular damage and regeneration experiments.

Germ cell transplantation and reconstitution

Donor cells were isolated from *Miwi2$^{Tom/+}$; Rosa26$^{YFP/+}$* testis by FACS and sorted in PBS/10% FCS as described above without the addition of sodium azide. 10^4 Miwi2-Tom^{HI}, c-kit^{Neg} FACS-sorted cells were resuspended in a volume of 10 µl in fresh DMEM/0.05% Trypan blue for injection. The unsorted control cells (10^6) were isolated from testicular cell suspensions passed through the FACS, but not sorted using any parameters except for viability such that the cells have undergone the same treatment as the Tom^{HI}, c-kit^{Neg} cells. The injection glass pipet was previously prepared by pulling 3-inch long borosilicate glass with a 1-mm outer diameter (World Precision Instruments # TW100-3) in a P-1000 pipette puller (Sutter Instruments). The tip of each pipette was ground to a sharp 40 degree beveled point on an EG-45 Microgrinder (Narishige Group). Before the injection, the pipette was loaded with cells and secured in a micropipette-holder (WPI Instruments) and used for delivery of the various cell populations. Surgery was performed under isoflurane–oxygen vapor anesthesia. The capillary needle was gently inserted into the rete-testis through the efferent duct of the recipient animal, and ∼10 µl of the cell solution was transplanted. The injection filled 75–85% of the tubules in each recipient testis. 50 µg anti-CD4 antibody (GK1.5)

was intraperitoneally injected to recipient mice on days 0, 2, and 4 after transplantation to prevent potential immune rejection. To assay transplantation, recipient mouse testes were recovered ∼11 wk after surgery and analyzed by observing the number of YFP fluorescent colonies formed. A cluster of germ cells was defined as a colony when it occupied the entire circumference of the tubule and was at least 0.1 mm long. Testes were then OCT embedded and frozen immediately. They were then cut in to 7-µm-thick slices and stained with α-GFP (Invitrogen) and α-GFRα1 (R&D Systems) antibody as described above.

Statistical analysis

An unpaired two-tailed Student's *t* test was used for all statistical analysis.

Online supplemental material

Fig. S1 shows the validation of the *Miwi2*$^{tdTomato/+}$ allele, as well as FACS analysis of the adult Miwi2-Tom^{Pos}c-kit^{Pos} cells. Fig. S2 shows the *Miwi2*$^{DTR/+}$ allele and the FACS after one DTx injection and 8 wk after three Dtx injections. Fig. S3 shows the regeneration experiment with Busulfan administered before the three Dtx injections.

ACKNOWLEDGMENTS

We are very grateful to Elena Vicini for technical advice on transplantation. The Miwi2$^{tdTomato/+}$ and Miwi2$^{DTR/+}$ alleles will be freely available on a non-collaborative basis.

The research leading to these results has received funding from the European Research Council under the European Union's Seventh Framework Program (*FP7/2007-2013*)/ERC grant agreement no. GA 310206. This study was technically supported by of EMBL's genomic core facility, as well as EMBL Monterotondo's FACS and microscopy core facilities.

The authors declare no competing financial interests.

Submitted: 20 August 2016

Revised: 3 February 2017

Accepted: 17 March 2017

REFERENCES

Aloisio, G.M., Y. Nakada, H.D. Saatcioglu, C.G. Peña, M.D. Baker, E.D. Tarnawa, J. Mukherjee, H. Manjunath, A. Bugde, A.L. Sengupta, et al. 2014. PAX7 expression defines germline stem cells in the adult testis. *J. Clin. Invest.* 124:3929–3944. http://dx.doi.org/10.1172/JCI75943

Aravin, A.A., R. Sachidanandam, D. Bourc'his, C. Schaefer, D. Pezic, K.F. Toth, T. Bestor, and G.J. Hannon. 2008. A piRNA pathway primed by individual transposons is linked to de novo DNA methylation in mice. *Mol. Cell.* 31:785–799. http://dx.doi.org/10.1016/j.molcel.2008.09.003

Brawley, C., and E. Matunis. 2004. Regeneration of male germline stem cells by spermatogonial dedifferentiation in vivo. *Science.* 304:1331–1334. http://dx.doi.org/10.1126/science.1097676

Buaas, F.W., A.L. Kirsh, M. Sharma, D.J. McLean, J.L. Morris, M.D. Griswold, D.G. de Rooij, and R.E. Braun. 2004. Plzf is required in adult male germ cells for stem cell self-renewal. *Nat. Genet.* 36:647–652. http://dx.doi.org/10.1038/ng1366

Busch, K., K. Klapproth, M. Barile, M. Flossdorf, T. Holland-Letz, S.M. Schlenner, M. Reth, T. Höfer, and H.-R. Rodewald. 2015. Fundamental properties of unperturbed haematopoiesis from stem cells in vivo. *Nature.* 518:542–546. http://dx.doi.org/10.1038/nature14242

Buza-Vidas, N., M. Cheng, S. Duarte, H.N. Charoudeh, S.E.W. Jacobsen, and E. Sitnicka. 2009. FLT3 receptor and ligand are dispensable for maintenance and posttransplantation expansion of mouse hematopoietic stem cells. *Blood.* 113:3453–3460. http://dx.doi.org/10.1182/blood-2008-08-174060

Carmell, M.A., A. Girard, H.J.G. van de Kant, D. Bourc'his, T.H. Bestor, D.G. de Rooij, and G.J. Hannon. 2007. MIWI2 is essential for spermatogenesis and repression of transposons in the mouse male germline. *Dev. Cell.* 12:503–514. http://dx.doi.org/10.1016/j.devcel.2007.03.001

Chan, F., M.J. Oatley, A.V. Kaucher, Q.-E. Yang, C.J. Bieberich, C.S. Shashikant, and J.M. Oatley. 2014. Functional and molecular features of the Id4+ germline stem cell population in mouse testes. *Genes Dev.* 28:1351–1362. http://dx.doi.org/10.1101/gad.240465.114

Chen, C., W. Ouyang, V. Grigura, Q. Zhou, K. Carnes, H. Lim, G.-Q. Zhao, S. Arber, N. Kurpios, T.L. Murphy, et al. 2005. ERM is required for transcriptional control of the spermatogonial stem cell niche. *Nature.* 436:1030–1034. http://dx.doi.org/10.1038/nature03894

Costoya, J.A., R.M. Hobbs, M. Barna, G. Cattoretti, K. Manova, M. Sukhwani, K.E. Orwig, D.J. Wolgemuth, and P.P. Pandolfi. 2004. Essential role of Plzf in maintenance of spermatogonial stem cells. *Nat. Genet.* 36:653–659. http://dx.doi.org/10.1038/ng1367

De Fazio, S., N. Bartonicek, M. Di Giacomo, C. Abreu-Goodger, A. Sankar, C. Funaya, C. Antony, P.N. Moreira, A.J. Enright, and D. O'Carroll. 2011. The endonuclease activity of Mili fuels piRNA amplification that silences LINE1 elements. *Nature.* 480:259–263. http://dx.doi.org/10.1038/nature10547

Farley, F.W., P. Soriano, L.S. Steffen, S.M. Dymecki, S. Przibilla, M. Noureddine, and M. Lezzi. 2000. Widespread recombinase expression using FLPeR (flipper) mice. *Genesis.* 28:106–110. http://dx.doi.org/10.1002/1526-968X(200011/12)28:3/4<106::AID-GENE30>3.0.CO;2-T

Grover, A., A. Sanjuan-Pla, S. Thongjuea, J. Carrelha, A. Giustacchini, A. Gambardella, I. Macaulay, E. Mancini, T.C. Luis, A. Mead, et al. 2016. Single-cell RNA sequencing reveals molecular and functional platelet bias of aged haematopoietic stem cells. *Nat. Commun.* 7:11075. http://dx.doi.org/10.1038/ncomms11075

Hara, K., T. Nakagawa, H. Enomoto, M. Suzuki, M. Yamamoto, B.D. Simons, and S. Yoshida. 2014. Mouse spermatogenic stem cells continually interconvert between equipotent singly isolated and syncytial states. *Cell Stem Cell.* 14:658–672. http://dx.doi.org/10.1016/j.stem.2014.01.019

Helsel, A.R., Q.-E. Yang, M.J. Oatley, T. Lord, F. Sablitzky, and J.M. Oatley. 2017. ID4 levels dictate the stem cell state in mouse spermatogonia. *Development.* 144:624–634. http://dx.doi.org/10.1242/dev.146928

Hobbs, R.M., M. Seandel, I. Falciatori, S. Rafii, and P.P. Pandolfi. 2010. Plzf regulates germline progenitor self-renewal by opposing mTORC1. *Cell.* 142:468–479. http://dx.doi.org/10.1016/j.cell.2010.06.041

Huckins, C. 1971. The spermatogonial stem cell population in adult rats. I. Their morphology, proliferation and maturation. *Anat. Rec.* 169:533–557. http://dx.doi.org/10.1002/ar.1091690306

Ikami, K., M. Tokue, R. Sugimoto, C. Noda, S. Kobayashi, K. Hara, and S. Yoshida. 2015. Hierarchical differentiation competence in response to retinoic acid ensures stem cell maintenance during mouse spermatogenesis. *Development.* 142:1582–1592. http://dx.doi.org/10.1242/dev.118695

Kanatsu-Shinohara, M., S. Toyokuni, and T. Shinohara. 2004. CD9 is a surface marker on mouse and rat male germline stem cells. *Biol. Reprod.* 70:70–75. http://dx.doi.org/10.1095/biolreprod.103.020867

Kubota, H., M.R. Avarbock, and R.L. Brinster. 2003. Spermatogonial stem cells share some, but not all, phenotypic and functional characteristics

with other stem cells. *Proc. Natl. Acad. Sci. USA.* 100:6487–6492. http://dx.doi.org/10.1073/pnas.0631767100

Kuramochi-Miyagawa, S., T. Watanabe, K. Gotoh, Y. Totoki, A. Toyoda, M. Ikawa, N. Asada, K. Kojima, Y. Yamaguchi, T.W. Ijiri, et al. 2008. DNA methylation of retrotransposon genes is regulated by Piwi family members MILI and MIWI2 in murine fetal testes. *Genes Dev.* 22:908–917. http://dx.doi.org/10.1101/gad.1640708

Livak, K.J., and T.D. Schmittgen. 2001. Analysis of relative gene expression data using real-time quantitative PCR and the $2^{-\Delta\Delta C_T}$ method. *Methods.* 25:402–408. http://dx.doi.org/10.1006/meth.2001.1262

Metcalfe, C., N.M. Kljavin, R. Ybarra, and F.J. de Sauvage. 2014. Lgr5+ stem cells are indispensable for radiation-induced intestinal regeneration. *Cell Stem Cell.* 14:149–159. http://dx.doi.org/10.1016/j.stem.2013.11.008

Nakagawa, T., Y. Nabeshima, and S. Yoshida. 2007. Functional identification of the actual and potential stem cell compartments in mouse spermatogenesis. *Dev. Cell.* 12:195–206. http://dx.doi.org/10.1016/j.devcel.2007.01.002

Nakagawa, T., M. Sharma, Y. Nabeshima, R.E. Braun, and S. Yoshida. 2010. Functional hierarchy and reversibility within the murine spermatogenic stem cell compartment. *Science.* 328:62–67. http://dx.doi.org/10.1126/science.1182868

Naughton, C.K., S. Jain, A.M. Strickland, A. Gupta, and J. Milbrandt. 2006. Glial cell-line derived neurotrophic factor-mediated RET signaling regulates spermatogonial stem cell fate. *Biol. Reprod.* 74:314–321. http://dx.doi.org/10.1095/biolreprod.105.047365

Oakberg, E.F. 1971. Spermatogonial stem-cell renewal in the mouse. *Anat. Rec.* 169:515–531. http://dx.doi.org/10.1002/ar.1091690305

Oatley, J.M., M.R. Avarbock, A.I. Telaranta, D.T. Fearon, and R.L. Brinster. 2006. Identifying genes important for spermatogonial stem cell self-renewal and survival. *Proc. Natl. Acad. Sci. USA.* 103:9524–9529. http://dx.doi.org/10.1073/pnas.0603332103

Palakodeti, D., M. Smielewska, Y.-C. Lu, G.W. Yeo, and B.R. Graveley. 2008. The PIWI proteins SMEDWI-2 and SMEDWI-3 are required for stem cell function and piRNA expression in planarians. *RNA.* 14:1174–1186. http://dx.doi.org/10.1261/rna.1085008

Reddien, P.W., N.J. Oviedo, J.R. Jennings, J.C. Jenkin, and A. Sánchez Alvarado. 2005. SMEDWI-2 is a PIWI-like protein that regulates planarian stem cells. *Science.* 310:1327–1330. http://dx.doi.org/10.1126/science.1116110

Reding, S.C., A.L. Stepnoski, E.W. Cloninger, and J.M. Oatley. 2010. THY1 is a conserved marker of undifferentiated spermatogonia in the pre-pubertal bull testis. *Reproduction.* 139:893–903. http://dx.doi.org/10.1530/REP-09-0513

Sada, A., A. Suzuki, H. Suzuki, and Y. Saga. 2009. The RNA-binding protein NANOS2 is required to maintain murine spermatogonial stem cells. *Science.* 325:1394–1398. http://dx.doi.org/10.1126/science.1172645

Saito, M., T. Iwawaki, C. Taya, H. Yonekawa, M. Noda, Y. Inui, E. Mekada, Y. Kimata, A. Tsuru, and K. Kohno. 2001. Diphtheria toxin receptor-mediated conditional and targeted cell ablation in transgenic mice. *Nat. Biotechnol.* 19:746–750. http://dx.doi.org/10.1038/90795

Shinohara, T., M.R. Avarbock, and R.L. Brinster. 1999. β_1- and α_6-integrin are surface markers on mouse spermatogonial stem cells. *Proc. Natl. Acad. Sci. USA.* 96:5504–5509. http://dx.doi.org/10.1073/pnas.96.10.5504

Shinohara, T., K.E. Orwig, M.R. Avarbock, and R.L. Brinster. 2000. Spermatogonial stem cell enrichment by multiparameter selection of mouse testis cells. *Proc. Natl. Acad. Sci. USA.* 97:8346–8351. http://dx.doi.org/10.1073/pnas.97.15.8346

Sun, F., Q. Xu, D. Zhao, and C. Degui Chen. 2015. Id4 Marks Spermatogonial Stem Cells in the Mouse Testis. *Sci. Rep.* 5:17594. http://dx.doi.org/10.1038/srep17594

Tata, P.R., H. Mou, A. Pardo-Saganta, R. Zhao, M. Prabhu, B.M. Law, V. Vinarsky, J.L. Cho, S. Breton, A. Sahay, et al. 2013. Dedifferentiation of committed epithelial cells into stem cells in vivo. *Nature.* 503:218–223.

van Es, J.H., T. Sato, M. van de Wetering, A. Lyubimova, A.N.Y. Nee, A. Gregorieff, N. Sasaki, L. Zeinstra, M. van den Born, J. Korving, et al. 2012. Dll1+ secretory progenitor cells revert to stem cells upon crypt damage. *Nat. Cell Biol.* 14:1099–1104. http://dx.doi.org/10.1038/ncb2581

van Keulen, C.J., and D.G. de Rooij. 1973. Spermatogonial stem cell renewal in the mouse. II. After cell loss. *Cell Tissue Kinet.* 6:337–345.

Wilson, A., E. Laurenti, G. Oser, R.C. van der Wath, W. Blanco-Bose, M. Jaworski, S. Offner, C.F. Dunant, L. Eshkind, E. Bockamp, et al. 2008. Hematopoietic stem cells reversibly switch from dormancy to self-renewal during homeostasis and repair. *Cell.* 135:1118–1129. http://dx.doi.org/10.1016/j.cell.2008.10.048

Yoshinaga, K., S. Nishikawa, M. Ogawa, S. Hayashi, T. Kunisada, T. Fujimoto, and S. Nishikawa. 1991. Role of c-kit in mouse spermatogenesis: identification of spermatogonia as a specific site of c-kit expression and function. *Development.* 113:689–699.

Zheng, D., L. Yin, and J. Chen. 2014. Evidence for Scgb1a1(+) cells in the generation of p63(+) cells in the damaged lung parenchyma. *Am. J. Respir. Cell Mol. Biol.* 50:595–604. http://dx.doi.org/10.1165/rcmb.2013-0327OC

Zheng, K., X. Wu, K.H. Kaestner, and P.J. Wang. 2009. The pluripotency factor LIN28 marks undifferentiated spermatogonia in mouse. *BMC Dev. Biol.* 9:38. http://dx.doi.org/10.1186/1471-213X-9-38